Journal of Fusion Energy (2020) 39:194–201
https://doi.org/10.1007/s10894-020-00231-y

ORIGINAL RESEARCH

Theoretical Modeling of High-Resolution X-ray Spectra Emitted by Tungsten and Molybdenum Ions from Tokamak Plasmas

Ł. Syrocki[1] · K. Słabkowska[1] · E. Węder[1] · M. Polasik[1] · J. Rzadkiewicz[2]

Published online: 30 January 2020

Abstract
In order to allow the advanced interpretation of the X-ray spectra registered by the high-resolution crystal KX1 spectrometer on the JET with an ITER-like wall, especially to determine how the relative emission contributions of tungsten and molybdenum ions change during a JET discharge, the X-ray spectra have been carefully modeled over a narrow wavelength range. The simulations have been done in the framework of Collisional–Radiative model implemented in Flexible Atomic Code for an electron density ($n_e = 2.5 \times 10^{19}$ m^{-3}), and electron temperatures between $T_e = 3.0$ keV and $T_e = 4.5$ keV, typical for JET. Moreover, performed detailed analysis in the framework of the proposed procedure can be useful in determining temperature of a high temperature plasma generated in tokamaks.

Keywords X-ray spectra · Tokamak · Tungsten M X-ray lines · Molybdenum L X-ray lines · High-resolution crystal spectrometer

Introduction

The hot, low density plasma in a tokamak such as JET emits a very complex radiation spectrum over a wide range of photon energies; qualitatively the same is expected from the future thermonuclear reactor ITER. Plasma diagnostics based on spectra that compensate their modest energy resolution with a large energy range and the associated modeling [1–9] can be just as useful as the complementary approach, taken here and in an earlier paper [10], that interprets the details in the shape of a few overlapping lines in terms of the plasma parameters.

This paper shows how to determine the emission contributions from tungsten and molybdenum ions in X-ray spectra measured, in the specific wavelength region covered by the high-resolution crystal spectrometer KX1, which is local, JET specific assignment for the plasma parameters diagnostic [9–14]. As before [10], the analysis here applies to the plasmas that are test beds for ITER, notably the operating scenarios planned for JET with the ITER-like wall, and for the deuterium–tritium (DT) campaign. We demonstrate that, with careful analysis, a minute spectral region already contains sufficient information to determine certain plasma parameters for a high-temperature tokamak plasma.

"X-ray Spectra Simulations in the Framework of Collisional-Radiative Model" section describes briefly the X-ray spectra simulations in the framework of Collisional–Radiative (CR) model performed using Flexible Atomic Code (FAC) package [15]. The proposed procedure for determining the high temperature tokamak plasma parameters are presented in detail in "Procedure for Determining the High Temperature Tokamak Plasma Parameters" section. It requires the computation of the tungsten M X-ray lines and the molybdenum L X-ray lines for different electron temperatures. "Summary" section summarizes the results.

Over a wide range of electron temperature, the plasma in large tokamaks radiates intensely from the highly ionized tungsten ions between Cu-like and Co-like (i.e., W^{45+}, W^{46+} and W^{47+}); higher temperature results in higher ionization states and an obvious direct effect on the radiation spectrum [13]. In addition, in certain individual ion

✉ Ł. Syrocki
lukaszsyrocki@umk.pl

[1] Faculty of Chemistry, Nicolaus Copernicus University in Toruń, 87-100 Toruń, Poland

[2] National Centre for Nuclear Research, 05-400 Otwock, Poland

species the plasma temperature affects the subshell populations as well, resulting in changes to the spectrum that are more subtle. Their diagnostic possibilities were explored earlier in [9, 10], and are described further below. Only two tungsten ion charges are relevant here, Cu-like W^{45+} and Ni-like W^{46+}, and in addition the Ne-like impurity molybdenum ion Mo^{32+}.

The reason to analyze a minute (0.04 Å) spectral region further for its potential as a plasma diagnostic follows from the success in interpreting JET's crystal spectrometer KX1 high-resolution X-ray spectra previously [10, 11]. These studies show that the overall structure of the M X-ray spectra that comes from Ni-like (W^{46+}) tungsten ions remains substantially the same as the plasma electron temperature changes. However, the high-resolution spectra are reproduced properly only when the computations for Cu-like W^{45+} ions take into account separately the individual 4d → 3p transitions for the $4s^1$, $4p^1$, $4d^1$ and $4f^1$ occupied subshells. An unintended molybdenum impurity, which in considered wavelength is mainly Ne-like Mo^{32+}, radiates L-shell X-rays corresponding to 3s → 2p transitions that happen to fall right in between those of the M shell X-rays from Cu-like and Ni-like tungsten ions, a coincidence that offers a way to determine how much molybdenum is present in the JET plasma. This is done by creating a data base of spectral shapes, selection of relevant plasma parameters, and then interpreting high-resolution X-ray spectra in terms of these parameters.

X-ray Spectra Simulations in the Framework of Collisional–Radiative Model

The simulations are performed using the FAC package. It consists of three main components. In the non-plasma, atomic part of FAC a fully relativistic Dirac–Fock–Slater iteration method calculates atomic data, such as energy levels and transition probabilities for radiative transitions and auto-ionization. In addition, the FAC calculates cross sections for excitation and ionization by electron impact, and the inverse processes (e.g., radiative recombination and dielectronic capture). Within the CR approximation as appropriate for a hot, low density tokamak plasma [15–21], the FAC code estimates fractional ionizations from the atomic data for the relevant processes. Typically, these include: (a) electron–ion collisions (notably excitation and deexcitation, ionization and 3-body recombination, radiative recombination, and dielectronic capture); (b) ion–ion collisions (with charge exchange); and (c) radiative and atomic processes (notably spontaneous and stimulated radiative transitions, photoionization, photoexcitation, and autoionization). For the optically transparent tokamak plasma here, the corresponding rates can be pre-computed by convolving the cross sections with a Maxwellian electron energy distribution with the electron temperature T_e as the parameter, and with the electron and ion densities as appropriate. Finally, the calculation use the radiative rates to find the plasma's radiation spectrum per ion per unit time.

In these analyses the transport effects are neglected because the analyzed X-ray structures originating from ions W^{45+} and W^{46+} arise in the central JET plasma, which may be considered as a zone of reduced transport [22, 23]. The X-ray structures associated with Mo^{32+} ions may come from a volume that is slightly closer to the edge and thus may be more sensitive to the transport effects. However, in this case there is only one stage of Mo ionization (q = 32+), that is needed to deal with. Therefore, the intensities of both Mo^{32+} X-ray lines monitored by the KX1 diagnostic at JET are independent from the intensities of the W^{45+} and W^{46+} lines.

Procedure for Determining the High Temperature Tokamak Plasma Parameters

To determine the parameters, notably the temperature, of the plasma in a fusion reactor, we have to follow 3 particular stages of the procedure proposed in Ref. [9].

Stage I. Creation of a universal base of theoretical benchmarks for tungsten and molybdenum ions X-ray spectral shapes as presented in Figs. 1, 2 and 3.

Stage II. Determination and collection of a set of detailed values of contributions to the X-ray spectra registered for a known plasma temperature, obtained as a result of the decomposition into benchmarks accordingly with the stage I. Examples for the JET tokamak are in Figs. 4 and 5. The result is another set of benchmarks, i.e.,

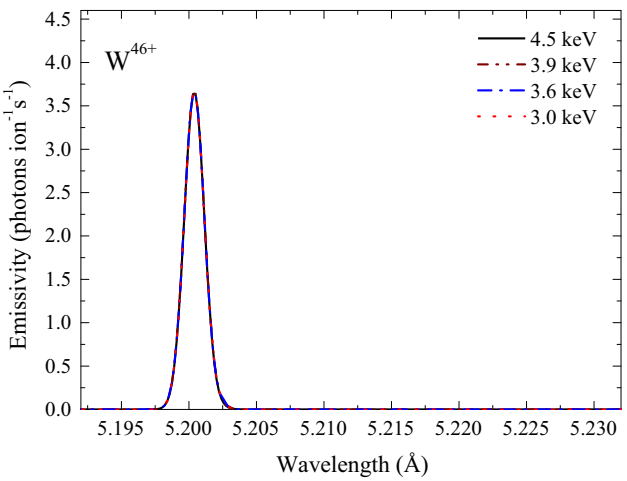

Fig. 1 The M X-ray line originating from $3p^54d^1$ → $3p^6$ transition type in Ni-like tungsten (W^{46+}) ions

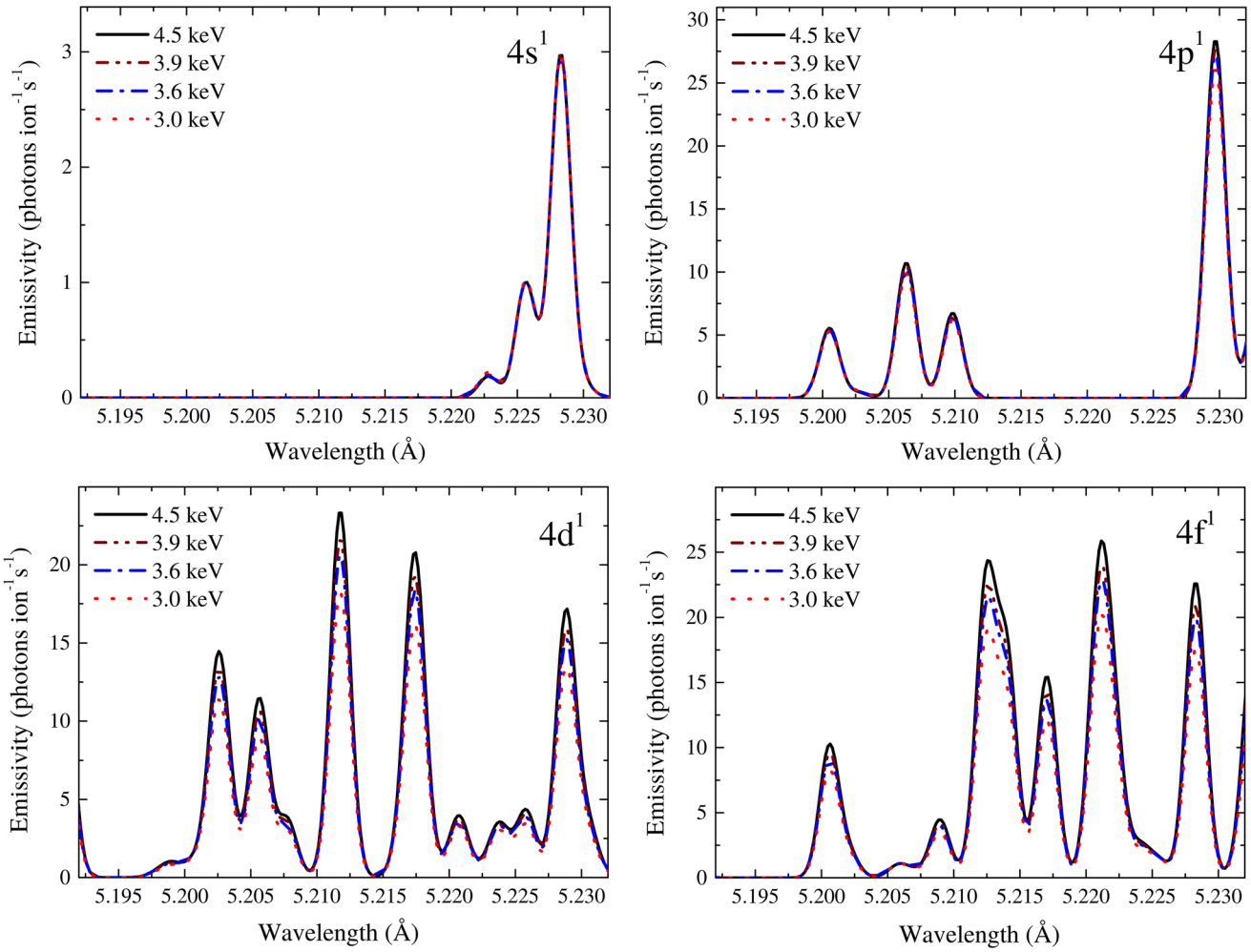

Fig. 2 The M X-ray line structure from the Cu-like tungsten (W^{45+}) ion for individual contributions of $3p^5 4s^1 4d^1 \rightarrow 3p^6 4s^1$, $3p^5 4p^1 4d^1 \rightarrow 3p^6 4p^1$, $3p^5 4d^2 \rightarrow 3p^6 4d^1$ and $3p^5 4d^1 4f^1 \rightarrow 3p^6 4f^1$ transition types (for the different temperatures-lines in color). The temperature visibly affects the line shapes for the $4d^1$ and $4f^1$ subshells only (Color figure online)

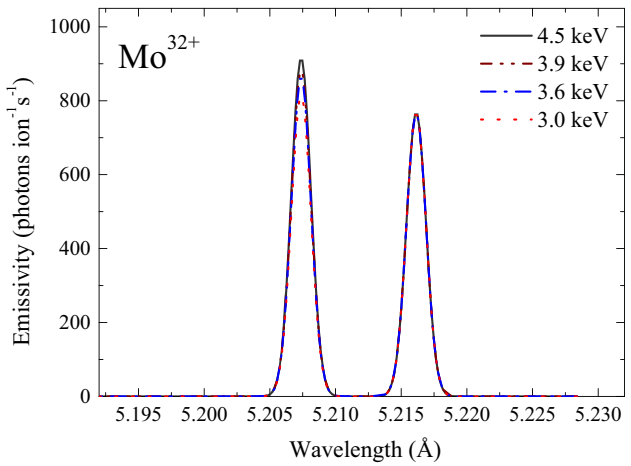

Fig. 3 The L X-ray lines spectrum for the $2p^5 3s^1 \rightarrow 2p^6$ transition type in Ne-like molybdenum (Mo^{32+}) ion

the relative contributions from tungsten (W^{46+} and W^{45+}), and the abundance ratio W^{46+}/W^{45+}, as well as the relative amount of molybdenum (Mo^{32+}) ions.

Stage III. Determination of the parameters for unknown plasma conditions by interpretation of high resolution X-ray spectra for given thermonuclear reactor. First, the contributions from tungsten (W^{46+} and W^{45+}) and molybdenum (Mo^{32+}) ions, and abundance ratios W^{46+}/W^{45+} of the plasma are identified through the decomposition of registered X-ray spectra. Then, the specific values of the plasma temperature is evaluated by fitting the details of the contributions from tungsten and molybdenum ions and abundance ratio W^{46+}/W^{45+} with those predicted as benchmarks in stage II. The present paper does not address this latter stage.

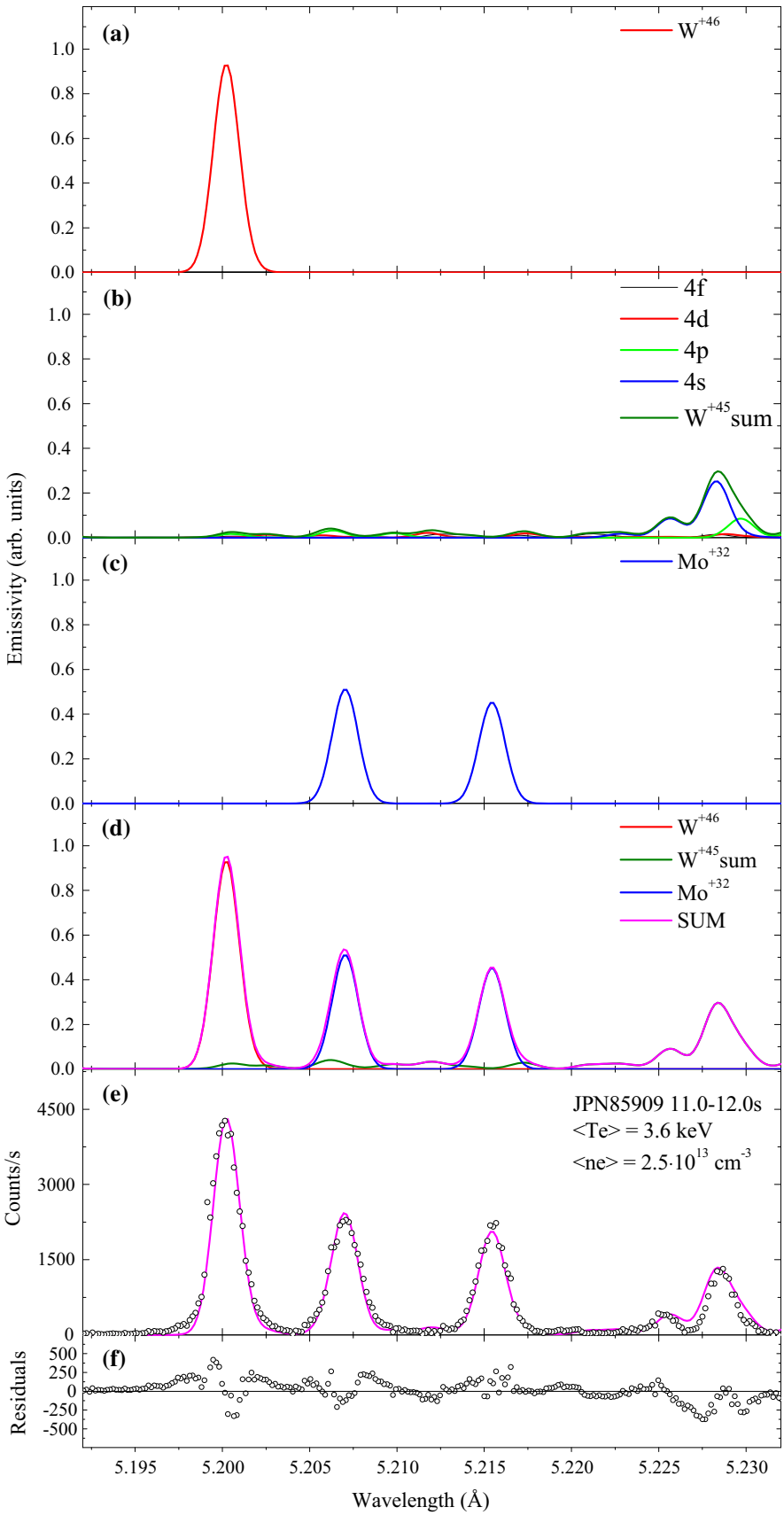

Fig. 4 The M X-ray line shapes in the wavelength range 5.192–5.232 Å, for Ni-like tungsten (W^{46+}) ion [panel (**a**)], separately for Cu-like tungsten (W^{45+}) ion [panel (**b**)], and the L X-ray lines for Ne-like molybdenum (Mo^{32+}) ion [panel (**c**)] with the relative ion abundancies for T_e = 3.6 keV (see text). Panel (**d**) is the superposition of the spectra (**a**), (**b**) and (**c**). Panel (**e**) is the experimental spectrum for similar parameters; panel (**f**) shows the residuals, i.e. the difference between the experimental and theoretical spectrum

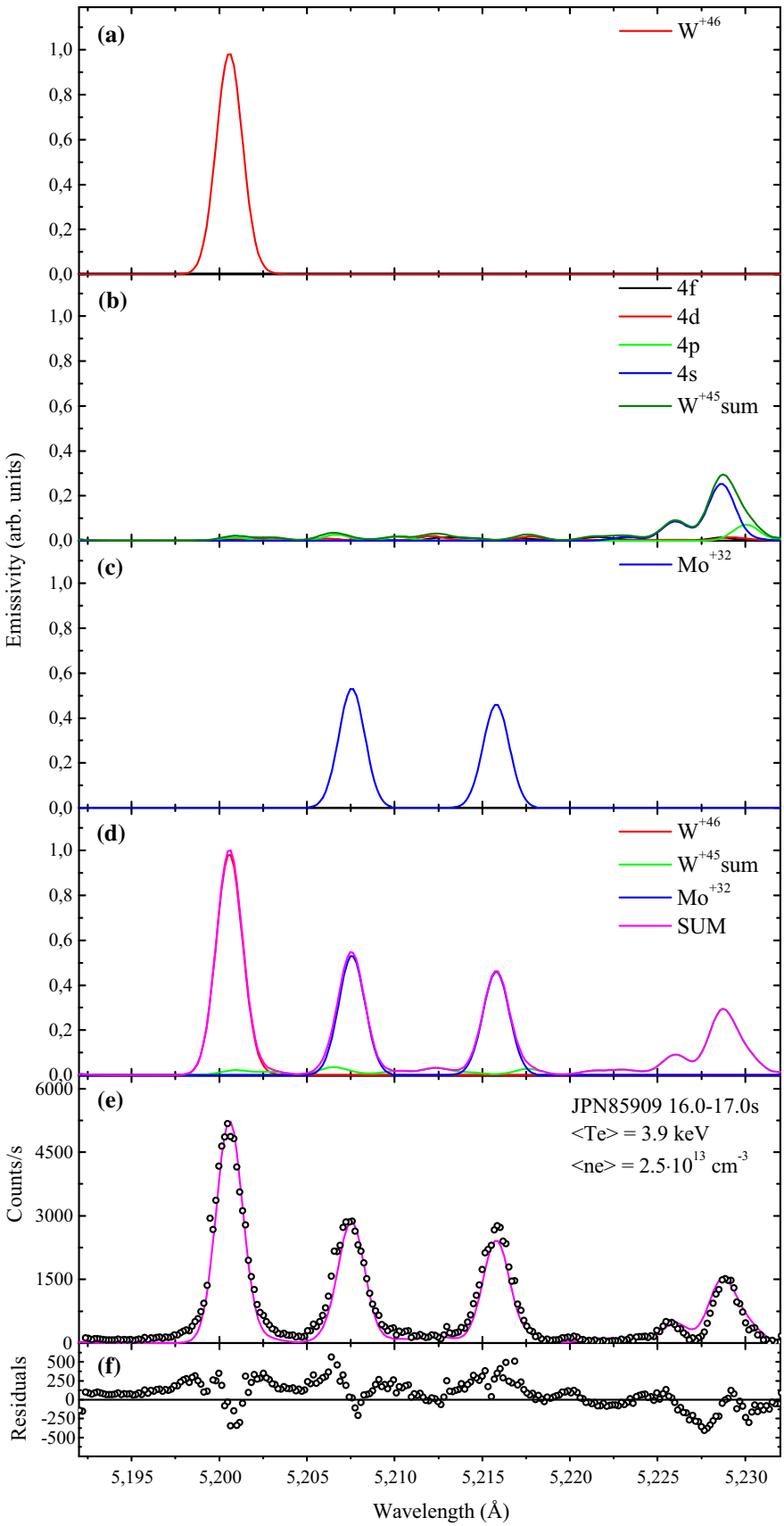

Fig. 5 The M X-ray line shapes in the wavelength range 5.192–5.232 Å, for Ni-like tungsten (W^{46+}) ion [panel (**a**)], separately for Cu-like tungsten (W^{45+}) ion [panel (**b**)], and the L X-ray lines for Ne-like molybdenum (Mo^{32+}) ion [panel (**c**)] with the relative ion abundancies for T_e = 3.9 keV (see text). Panel (**d**) is the superposition of the spectra (**a**), (**b**) and (**c**). Panel (**e**) is the experimental spectrum for similar parameters; panel (**f**) show the residuals, i.e. the difference between the experimental and theoretical spectrum

Benchmarks for Tungsten and Molybdenum Ions X-ray Spectral Shapes: Stage I

The relevant X-rays here are the M X-ray lines emitted by Ni-like tungsten (W^{46+}) ions, by the individual subshells in Cu-like tungsten (W^{45+}) ions, and the L-shell X-ray lines from Ne-like molybdenum (Mo^{32+}) ions. The radiation is computed for the 5.192–5.232 Å wavelength window (energy from 2.388 to 2.370 keV), which the KX1 spectrometer covers with a very high spectral resolution (better than $\lambda/\Delta\lambda = 12{,}000$ [24]). Our modeling uses a single electron density of 2.5×10^{19} m^{-3}, and electron temperatures between 3.0 and 4.5 keV as is typical for the JET tokamak.

As can be seen in Fig. 1, the M X-ray line originating from tungsten W^{46+} ions for transitions $3p^5 4d^1 \rightarrow 3p^6$ is a single peak at 5.201 Å. Neither the shape of this peak nor its emissivity changes visibly as the electron temperature increases within the considered range (from 3.0 to 4.5 keV).

The previous analysis, presented in Refs. [9, 10], already showed that reproducing high resolution spectra demands a separate accounting of the contributions from the $4s^1$, $4p^1$, $4d^1$ and $4f^1$ subshell states of Cu-like tungsten. Figure 2 contains the individual contributions to the M X-ray line structures from these tungsten W^{45+} ions. Their shapes differ significantly from each other, hence (as in Refs. [9, 10]), for tungsten W^{45+} ions it is clearly important which subshell is occupied. The wavelengths of the various peaks are uniquely determined by the ion's specific ionization stage and therefore do not depend on the temperature. Instead, for W^{45+} the structure of the total spectrum changes with temperature because for some of the subshells the temperature affects the individual peak's emissivity. The electron temperature has almost no effect on the radiation from the $4s^1$, which in addition, has an order of magnitude lower emissivity than the other subshells. For the $4p^1$ subshell the largest peak is at 5.231 Å and 0.02 Å (12 eV) apart from the three overlapping peaks in the center of the wavelength range. The emissivity of this peak increases with the electron temperature much more than the less intense peaks but the general appearance remains the same.

However, the temperature has a substantial influence on the spectrum from Cu-like tungsten W^{45+} when the transitions occur from the $4d^1$ and $4f^1$ subshell states, the bottom two panels in Fig. 2. Both spectra have 5 major peaks but they differ substantially in their complex structure. They cover the entire wavelength region from 5.192 to 5.232 Å. Here the emissivity clearly increases with electron temperature and, causes a noticeable change in the shape of the spectrum.

Figure 3 shows the spectrum for Ne-like molybdenum (Mo^{32+}) ions from $2p^5 3s^1 \rightarrow 2p^6$ transitions, again for temperatures from 3.0 to 4.5 keV. This L X-ray molybdenum spectrum consist of a peak at about 5.207 Å, well-separated (by 4 eV) from a second peak at about 5.216 Å. The emissivity of the first peak increases with electron temperature, but the second peak does not. Hence, the emissivity ratio is temperature-dependent and can serve as additional electron temperature verification.

Determination of the Contributions from Tungsten and Molybdenum Ions by Interpretation of the High Resolution X-ray Spectra Registered on JET: Stage II

Figures 4 and 5 compare the theoretically modeled structures of the tungsten M X-ray lines (in the top panels) and the molybdenum L X-ray lines with the experimental spectra (panels (e)). Panel 4(e) is the spectrum at the 12 s into JET Pulse Number (JPN) 85909 (averaged over 1s from 11 to 12 s); panel 5(e) is for the 17 s into the same JPN (averaged from 16 to 17 s). Panels 4(f) and 5(f) give the residues, i.e., the discrepancies between the observed and modeled spectra. The plasma parameters to model these JPNs are an electron density of $n_e = 2.5 \times 10^{19}$ m^{-3} and the two electron temperatures $T_e = 3.6$ keV (for the earlier time, in Fig. 4) and $T_e = 3.9$ keV (for the later time, in Fig. 5), which come from the LIDAR Thomson scattering diagnostic at JET [25].

Figures 4 and 5 show in detail how the individual W^{46+}, W^{45+} and Mo^{32+} ionization stages contribute to the final modeled X-ray spectra. The individual contributions are assumed to reproduce the measured spectra for the applicable electron temperatures 3.6 keV and 3.9 keV. In both cases the Ni-like tungsten W^{46+} ion is the most abundant (35.7% and 37.2%, respectively), so that this ion supplies the strongest line: its amplitude is near unity in panel (a). The more interesting spectrum is for the Cu-like tungsten (W^{45+}) ion in panel (b), which shows the summarized spectrum with the different assumed contributions from the individual states with filled $4s^1$, $4p^1$, $4d^1$, $4f^1$ subshells. It is worth noting, in panel (b), that the successful reproduction of experimental spectra remains possible when the dominant contribution is derived from the states 4s (13.9% and 13.7%) and 4p (6.3% and 5.0%) with smaller contributions from the states 4d (3.9% and 3.7%) and 4f (3.5% and 3.2%). In addition to the tungsten lines, the (36.7% and 37.2%) contribution from Ne-like L-shell of molybdenum (panel (c)) is needed to account for the two lines in the middle of the wavelength range; here the radiation from Cu-like tungsten can contribute only a minute amount that is restricted by the spectrum around 5.230 Å.

Panels (f) in Figs. 4 and 5 are the residues, the difference between the experimental and theoretical spectra. For both temperatures the residues are within 5% of the peak spectrum, only slightly larger than an estimated few-% of random noise to the residue. The residue may be relatively large where the spectrum is the least intense at a particular wavelength and difficult to interpret as a discrepancy, except for around 5.228 Å where the residue seems to be meaningful. Still, there is excellent overall agreement between the spectra measured over a 1s long period along a line across JET's not quite uniform plasma, and those computed for a comparable plasma with uniform density plasma at one specific temperature.

The analysis determines the abundance ratio W^{46+}/W^{45+} from the contributions to the total spectrum of the radiation from the W^{46+} and W^{45+} ions individually. For the lower plasma temperature, T_e = 3.6 keV W^{46+}/W^{45+} is about 1.29, increasing to 1.45 at the higher temperature T_e = 3.9 keV. As is seen directly from Fig. 5, which shows a higher relative contribution from the M X-ray line of the Ni-like tungsten W^{46+} ion. It is needed to underline that the authors were able to compare our abundance ratio W^{46+}/W^{45+} = 1.45 for higher electron temperature with the independent theoretical estimation of abundance ratio obtained using the ADAS package modified by Pütterich et al. [1] and Summers [26], which is equal to 1.4 as presented in the paper [11]. This comparison indicates excellent agreement between both theoretical predictions.

Summary

The X-ray spectrum measured with high resolution by the KX1 crystal spectrometer on JET over a narrow 0.04 Å wavelength range around 5.212 Å (2.379 keV) has been modeled accurately with the FAC code. The simulations are done for a typical JET plasma electron density ($n_e = 2.5 \times 10^{19}$ m^{-3}), and electron temperatures between T_e = 3.0 keV and T_e = 4.5 keV. For satisfactory modeling of the spectra from JPN 85909 at 12 s and 17 s into the discharge, the computations need to take into account only Cu-like and Ni-like tungsten, and the Ne-like ionization state of the molybdenum impurity. The modeled spectrum matches the experimental one very well but only when individual subshells of Cu-like tungsten are properly taken into account, and the right amount of the unintended molybdenum impurity radiation is added to simulated spectra. Moreover, performed detailed analysis in the framework of the proposed procedure can be useful in determining temperature of a high temperature plasma generated in tokamaks.

Acknowledgments This work has been carried out within the framework of the EUROfusion Consortium and has received funding from the Euratom research and training programme 2014–2019 under grant agreement No. 633053. The views and opinions expressed herein do not necessarily reflect those of the European Commission. This work was also supported by the National Science Centre (NCN), Poland under Grant No. 2017/25/B/ST2/00901. We thank Nino R. Pereira for editorial suggestions.

References

1. T. Pütterich, R. Neu, R. Dux, A.D. Whiteford, M.G. O'Mullane, Plasma Phys. Control. Fusion **50**, 085016 (2008)
2. P. Beiersdorfer, J.K. Lepson, M.B. Schneider, M.P. Bode, Phys. Rev. A **86**, 012509 (2012)
3. Y. Podpaly, J. Clementson, P. Beiersdorfer, J. Williamson, G.V. Brown, M.F. Gu, Phys. Rev. A **80**, 052504 (2009)
4. P. Beiersdorfer, J. Clementson, J. Dunn, J. Phys. B: At. Mol. Opt. Phys. **43**, 144008 (2010)
5. R. Neu, K.B. Fournier, D. Bolshukhin, R. Dux, Phys. Scr. **T92**, 307 (2001)
6. J. Clementson, P. Beiersdorfer, E.W. Magee, H.S. McLean, R.D. Wood, J. Phys. B: At. Mol. Opt. Phys. **43**, 144009 (2010)
7. Y. Ralchenko, I.N. Draganić, D. Osin, J.D. Gillaspy, J. Reader, Phys. Rev. A **83**, 032517 (2011)
8. J. Clementson, P. Beiersdorfer, Phys. Rev. A **81**, 052509 (2010)
9. K. Słabkowska, Ł. Syrocki, E. Węder, M. Polasik, Nucl. Instrum. Methods B **408**, 265 (2017)
10. K. Słabkowska, J. Rzadkiewicz, Ł. Syrocki, E. Szymańska, A. Shumack, M. Polasik, N.R. Pereira, JET contributors. J. Phys. B: At. Mol. Opt. Phys. **48**, 144028 (2015)
11. J. Rzadkiewicz et al., Phys. Rev. A **97**, 052501 (2018)
12. T. Nakano et al., J. Phys. B: At. Mol. Opt. Phys. **48**, 124023 (2015)
13. K. Słabkowska, M. Polasik, E. Szymańska, J. Starosta, Ł. Syrocki, J. Rzadkiewicz, N.R. Pereira, Phys. Scr. **T161**, 014015 (2014)
14. K. Słabkowska, M. Polasik, Ł. Syrocki, E. Szymańska, J. Rzadkiewicz, N.R. Pereira, J. Phys: Conf. Ser. **583**, 012031 (2015)
15. M.F. Gu, Can. J. Phys. **86**, 675 (2008)
16. R.W. Lee, J.K. Nash, Y. Ralchenko, J. Quant. Spectrosc. Radiat. Transf. **58**, 737 (1997)
17. C. Bowen, R.W. Lee, Y. Ralchenko, J. Quant. Spectrosc. Radiat. Transf. **99**, 102 (2006)
18. C.J. Fontes et al., High Energy Density Phys. **5**, 15 (2009)
19. S. Hansen et al., High Energy Density Phys. **9**, 523 (2013)
20. H.-K. Chung et al., High Energy Density Phys. **9**, 645 (2013)
21. J. Clementson, P. Beiersdorfer, G.V. Brown, M.F. Gu, Phys. Scr. **81**, 015301 (2010)
22. A. Langenberg et al., Nucl. Fusion **57**, 086013 (2017)

23. A. Czarnecka et al., Plasma Phys. Control. Fusion **53**, 035009 (2011)
24. A.E. Shumack et al., Rev. Sci. Instrum. **85**, 11E425 (2014)
25. C.W. Gowers, B.W. Brown, H. Fajemirokun, P. Nielsen, Y. Nizienko, B. Schunke, Rev. Sci. Instrum. **66**, 471 (1995)
26. H.P. Summers, *The ADAS User Manual, Version 2.6* (2004)